Multiple Uplinks Per Antenna (MUPA) Signal Acquisition Schemes

David D. Morabito[a] and Douglas S. Abraham[b]
Jet Propulsion Laboratory, California Institute of Technology, Pasadena, Calif. 91109

The Deep Space Network (DSN) currently makes use of the technique of Multiple Spacecraft per Antenna (MSPA) where a single antenna is used to track multiple spacecraft downlinks within its beam, such as in the case of multiple spacecraft orbiting Mars at 8.4 GHz (X-band). It is desired to extend this technique to the uplink where a single station is used to send a signal to multiple spacecraft in order to make more efficient use of ground resources. This would be applicable to numerous smallsat constellations being considered for future missions or to future spacecraft at Venus, Mars, or more distant destinations that are all within the half-power beamwidth of a single 34-m diameter antenna. In one scheme, each spacecraft's command sequences would be time multiplexed onto a single uplink frequency. Each spacecraft would lock onto the uplink signal and would accept only commands intended for it via special identifier codes. Each spacecraft would also emit a downlink signal to the ground that is coherent with the uplink signal but would have its own allocated frequency channel and identifier information.

A couple of key challenges associated with using this technique need to be addressed. Because of the single uplink frequency, coherent turnaround for two-way Doppler and ranging would not conform to established ratios, thus the radios employed by the spacecraft would need to be capable of variable turnaround ratios. In addition, because of the different orbits or spacecraft trajectories, the relative Doppler shifts and rates can be large with respect to the common uplink signal whose frequency would lie at the centroid of the frequencies of the expected received signals of the constellation. This would be problematic with standard analog spacecraft radios whose acquisition bandwidths are relatively small (~1.7 kHz) relative to the large frequency offsets (~100 kHz) expected using the single frequency uplink technique.

With the advent of software defined radios (SDRs), signal frequency search algorithms can be utilized within the flight software and/or programmable hardware (e.g., FPGAs) that can easily acquire and track signals with large frequency offsets and varying dynamics. Such techniques could include FFT search algorithms, step-and-sweep search algorithms, or on-board frequency steering making use of trajectory vectors uplinked to each member spacecraft. Other challenges include mitigation of potential interference between received signals.

We have identified several software defined radios that are in different stages of development and whose key parameters have been tabulated. We have examined each radio's capabilities with respect to acquiring and tracking signals with large frequency offsets. Such analyses made use of previous studies supplemented with specially designed tests using both simulation tools and/or existing testbeds. We have compared signal acquisition times computed from provided algorithms along with measured values derived from tests using existing hardware and simulation tools for the purpose of conducting tradeoff studies between the various radio designs and software/firmware programming approaches.

I. Introduction

Given that there are currently multiple spacecraft in orbit around Mars, it is common practice to use a single 34-m diameter ground antenna to track the downlinks at 8.4 GHz (X-band). This is because the X-band beamwidth as

[a] Telecommunications Engineer, Telecommunications Architectures, 4800 Oak Grove Dr. Pasadena, Calif. 91109.
[b] Strategic and Systems Forecasting Lead, Interplanetary Network Directorate, 4800 Oak Grove Dr. Pasadena, Calif. 91109, AIAA Senior Member.

seen from a 34-m diameter antenna extends beyond the projected orbits about the disk of Mars as illustrated in Figure 1, thus allowing for the more efficient use of ground resources. For the date of this SOAP[1] image, Mars subtends about 2.4 mdeg (range distance = 1.07 AU). Here the X-band beamwidth is about 29 times larger than the disk of Mars, where we have assumed the X-band frequency to be 7.15 GHz, the uplink frequency allocation. The X-band half-power beamwidth ranges from 14 Mars diameters at the nearest Earth-Mars distance to about 70 Mars diameters at the furthest Earth-Mars distance.

Given a group of spacecraft that resides in close angular proximity to each other, they can share the same downlink station thus conserving ground resources. This technique known as Multiple Spacecraft Per Antenna (MSPA)[2] allows a single antenna to be used with receivers dedicated to each spacecraft that are tuned to each spacecraft's downlink frequency (see Figure 2). Such is the case with Mars, where there are five orbiters being considered for this study: Mars Reconnaissance Orbiter (MRO), Mars Odyssey (ODY), MAVEN (MVN), Mars Orbiter Mission (MOM) and Mars Express (MEX). Each of these spacecraft possess an X-band downlink and an X-band uplink channel.

We now discuss the prospect and complexities of multiple spacecraft sharing the same uplink signal from a single ground station. For commanding, each spacecraft makes use of a unique command "packet" ID, accepting only commands containing their own ID and dismissing others. Thus, a multiplexing algorithm can be employed for commanding.

For uplink carrier acquisition using a single frequency to multiple spacecraft, there is the problem that there could be high relative Doppler offsets between spacecraft rendering conventional techniques (e.g., sweeps around mid-point uplink frequency) impractical. This can be inferred upon inspection of the geometry depicted in Figure 1 where the multiple spacecraft have different orbits and in some cases are traveling in near opposite directions resulting in high relative Doppler shifts and dynamics.

For such constellations[c] that make use of a single uplink, standard sweep techniques used for most deep-space vehicles are not practical due to large Doppler offsets and Doppler rates. The standard sweep technique using a single ground uplink is also not practical for cubesat constellations perhaps after deployment such as in the proximity of the Moon given that there could be high Doppler offsets and rates due to relative dynamics between spacecraft trajectories.

There are several different approaches for carrier acquisition (away from the standard uplink sweep near the BLF) that could be made possible using specialized on-board processing.

Such techniques require that the spacecraft radios be fully programmable and utilize digital processing algorithms. One such technique would involve on-board automation in the spacecraft computer that makes use of uploaded trajectory and ground station location information to compute the Doppler-shifted uplink frequency on which to have the receiver tune and lock onto. A variant of this technique would involve uploading frequency predictions in which to tune the receiver during scheduled upcoming passes freeing the spacecraft computer from performing trajectory estimation of tuning predicts. Other such techniques make use of a broadband view of possible incoming signal range and use an FFT or step-and-sweep approach in which to locate the signal in frequency space and then attempt lock. There are several software defined radios that are currently being evaluated for MUPA. Among the SDR radios that have flown or are in development are the UST, Electra, Iris, and Frontier.

The Univeral Space Transponder (UST) is an SDR which is reprogrammable and makes use of parallel processing[4]. Flight units of the near-Earth Ka-band modulator version of the UST are currently being built for the NASA-ISRO SAR (NISAR) mission, scheduled to launch by 2021. Additionally, a version of the UST supporting UHF, X-band, and Ka-band is currently baselined for future Mars orbiters. This radio can be expanded to handle several different RF links (UHF, S, X and Ka bands).

Conventional radios such as the small deep space transponder (SDST) are currently flying (or have flown) on several deep space missions. The SDST has a wide front-end bandwidth to accommodate a multi-MHz-wide uplink ranging signal but lacks the capability to perform carrier signal searches over the large bandwidth. The SDST can track within a frequency offset of ±200 kHz; however, it only has an acquisition range of ±1.3 kHz (unaided)[3]. Here the term "aiding" refers to standard DSN practice to uplink at a frequency very close to the radio's best-lock frequency (BLF) since all deep space missions employ excellent trajectory bookkeeping. This is done using uplink frequency ramps that compensate for Doppler so by the time the signal arrives at the spacecraft, its frequency is very close to the receiver's BLF. Given this dependence on ground-aided signal acquisition, acquisition using FFT and step-and-sweep signal search techniques are impractical with this type of radio.

A radio design that scans about the received frequency uncertainty band that uses step-wise sweep tuning of the NCO such as performed by Electra[5] has been used on several space missions. Early pre-flight tests involving the Electra testbed have only been previously performed with frequency offsets of ~14 kHz[6]. We plan tests in which we

[c] A "constellation" can be a collection of spacecraft at a destination that may belong to different missions, and may or may not be involved in coordinated operations.

expect to exercise the Electra signal search algorithms for frequency uncertainty regions of up to 200 kHz. The Electra radio scans the uncertainty region about the expected received center frequency using a step-wise sweep, over a 50 kHz to 200 kHz window. This approach makes use of in-phase (I) and quadrature (Q) components that have been made digitally available to be processed.

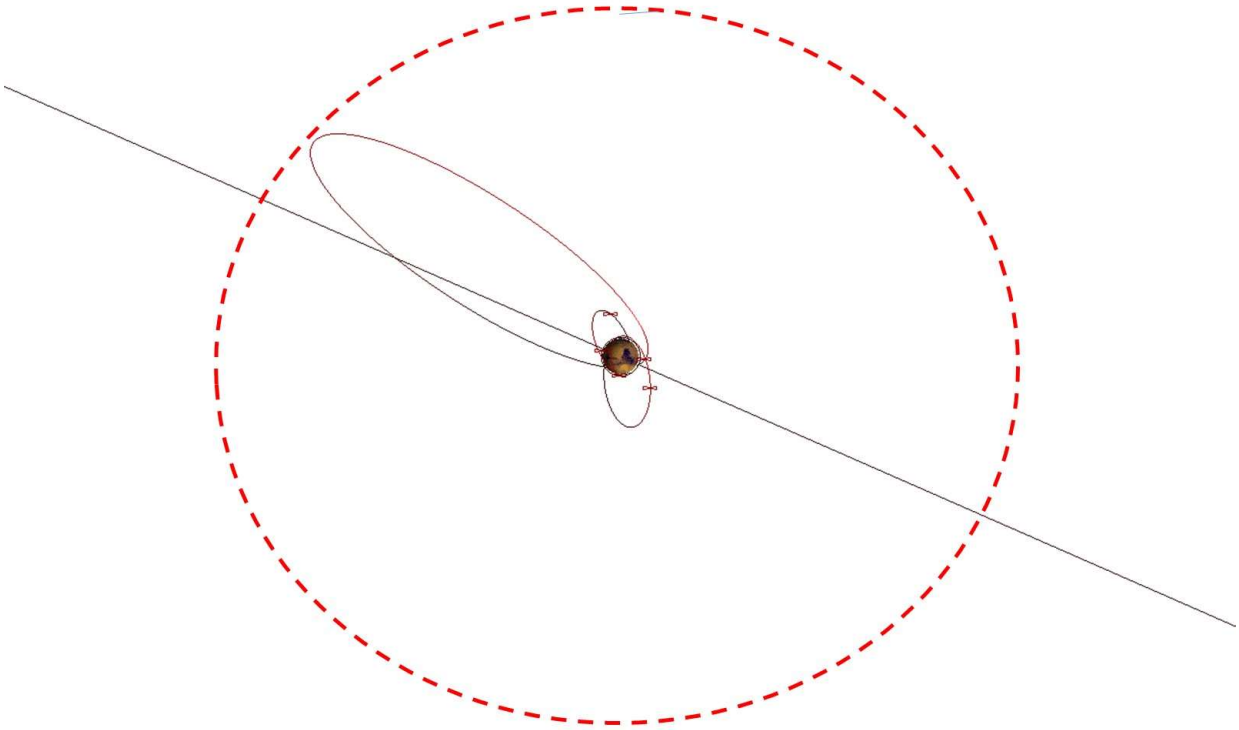

Figure 1 – SOAP[1] depiction of Mars shown with traces of orbits of five spacecraft currently in orbit around Mars. Also shown is the dashed red circle representing the approximate 3-dB end-to-end beamwidth of a 34-m DSN antenna at X-band centered at Mars when at a distance of 1.1 AU from the Earth.

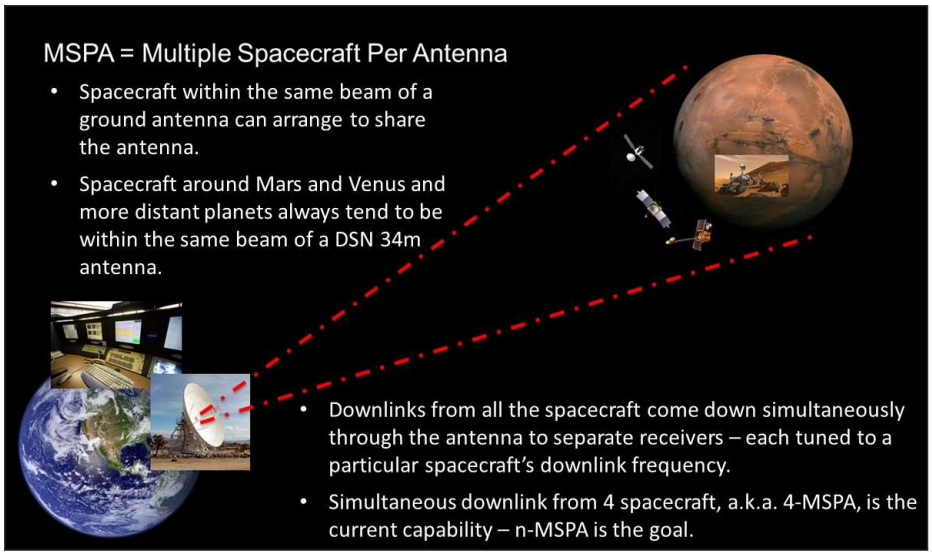

Figure 2 - Illustration of Multiple Spacecraft Per Antenna (MSPA) technique

The Iris radio is based on an architecture used for constructing highly reconfigurable radio networks[7]. These systems were developed using diverse processing platforms such as general-purpose processors and field-programmable gate arrays (FPGAs). This radio can provide support for all layers of the network stack and provides a user-friendly platform for development of cognitive radio networks. There are several missions that are planning to use or considering use of the Iris radio. Available testbeds that can "mimic" the Iris radio for developing and testing signal processing algorithms include the ML-605[8] and CoNNeCT[9].

The ML605 board enables developers to create or evaluate hardware and software designs targeting the Virtex®-6 FPGA, and possesses board features common to several processing systems. Additional features can be added through mezzanine cards.[8] One such feature useful for the signal acquisition study includes a mezzanine card that enables IF/RF functionality to allow signal acquisition testing via an appropriate environment with equivalent ground support equipment.

The STRS is a new generation of SDR technologies, and allows for development, testing and demonstration of new communications, networking, and navigation capabilities in a real space environment. It advances space communication technologies in support of future NASA missions and other U.S. space endeavors. The STRS is actually an architecture and standard. For instance, the prototype equipment that resides in the STRS testlab at JPL is built based on this architecture and standard, and it includes the CoNNeCT[10] prototype SDR and associated Ground Support Equipment (GSE). The flight model (FM) of the CoNNeCT radio is located aboard the International Space Station (ISS) where experiments can be carried out using an uplink signal from an antenna located at Glenn Research Center (GRC) and which generates a downlink signal that is received at an antenna located at GRC[11]. The CoNNeCT Engineering Model (EM) resides at GRC. The flight model of the CoNNeCT radio on-board the ISS is not expected to be available past FY2018.

The Frontier Radio is an SDR designed for spaceborne communications, navigation, radio science, and sensor applications. This radio was developed by the Johns Hopkins University Applied Physics Laboratory (JHU/APL). The Van Allen Probes mission was the first to make use of the Frontier Radio[12] thus providing flight heritage. A description of the radio being planned for Parker Solar Probe is found in[13-15], planned for launch in 2018. This radio uses software to allow enhancement of its digital signal processing capabilities, making testing to validate its features very complex[15].

II. Possible Scenarios for Multiple Uplinks from a Single Aperture

Several approaches for MUPA have been considered and will be discussed briefly here.

One non-simultaneous uplink method currently makes use of serial uplink swapping which allows each spacecraft to share a portion of the pass for uplink while 4-MSPA is occurring on the downlink (see Figure 3). This method allows for each spacecraft to obtain a portion of the total possible two-way Doppler and ranging, as well as commanding. However, within existing DSN prcedures, up to 30 minutes would be required during the handovers to each successive spacecraft between passes. This serial method could be improved upon if we could perform simultaneous uplinking to the multiple spacecraft

One approach to simultaneous uplinking involves using multiple exciters (multiple uplink frequencies) at the ground station that makes use of a single transmitter. This approach has the disadvantage in that it creates intermodulation products that exceed spectrum requirements. This approach would require an 80 kW transmitter to enable the power needed for the multiple exciters within a regime that is still linear. The Doppler shift is not an issue, since each ground exciter can be swept with respect to its associated spacecraft's anticipated Doppler shift. Thus, with this approach, there is no need for variable turnaround ratios.

A demonstration involving an uplink to Odyssey at 18 kW and an uplink to MRO at 5 kW yielded: (1) an intermodulation product at -28 dBc that was outside the X-band allocation and equivalent to 29W of radiated power, and (2) an intermodulation product at -33 dBc in the X-band near-Earth allocation equivalent to 9W of radiated power[d]. A linearizer might get these intermodulation products down another 6 to 10 dBc, but still would not meet the -60 dBc requirement[16]. This multiple exciter approach would be very complicated and expensive to implement for operational purposes. This approach would not be very practical for more than three simultaneous spacecraft supports.

Early tests were performed on a DSN 20 kW X-band (7.17 GHz) klystron amplifier uplink in order to characterize the intermodulation performance to a level of detail and accuracy not available from theoretical models[18]. The intermodulation products were characterized for up to three drive carriers of differing amplitude levels. These data could be used for frequency planning and frequency management in scenarios where multiple command signals are radiated simultaneously from a single antenna.

[d] T. Cornish (private communication), Jet Propulsion Laboratory, Pasadena, Calif., June 1, 2016.

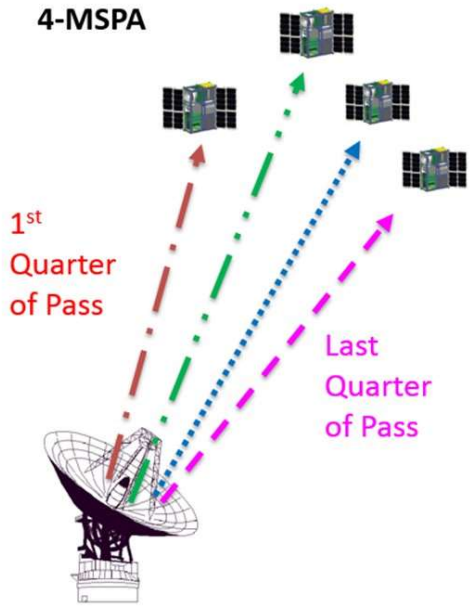

Figure 3 – Cartoon illustrating use of a single ground antenna performing serial uplinking to multiple spacecraft during a tracking pass.

A second approach would make use of multiple subcarriers modulated on a single carrier. A square wave can be used to modulate the multiple subcarriers onto the carrier. Each subcarrier will be a fixed frequency distance from the other, and each intended for one of the multiple spacecraft in the beam. This approach would require an 80 kW transmitter to provide adequate power at interplanetary distances. There is also potential for splattering of energy out of band, which would require careful consideration of filtering strategies and carrier placement. It would be difficult to accommodate the Doppler shift with this approach as one would be required to adjust the subcarrier spacing to accommodate the differential Doppler shifts. It is possible to achieve subcarrier spacing of MHz, or even tens of MHz, however staying in band becomes an issue. Supporting more than three spacecraft with this approach would not be feasible. The cost to demonstrate this approach is low but one would need to focus on one spacecraft and hope the other is able to lock up. The cost to implement this approach for operational use would be very high, but there would be no need for variable turnaround ratios.

The third and recommended approach would be to use a single uplink frequency with the commanding differentiated by spacecraft identification code. This approach would be easier to implement and is lower cost. Minor software changes would be required on ground, primarily in the handling of two-way Doppler and ranging. This approach would require variable turnaround ratios on the spacecraft radio. The frequency allocation process might require two uplink frequency assignments (one of them being the shared frequency). However, large differential Doppler shifts are problematic for sweeping and achieving lock, but are more manageable in this age of software defined radios and on-board digital signal processing.

One postulated case of using a single uplink signal from a single DSN station to a multiple-spacecraft constellation at Mars that was previously studied involved two aerostationary orbiters, an aerosynchronous orbiter, a human Deep Space Habitat (with a 48 h orbit) and a human landing site at Utopia Planitia[17]. This study proposed a new spacecraft receiver two-way tracking architecture that made use of uplinking a single frequency to the multiple spacecraft, employing a PLL with sweeping frequency to coherently acquire and estimate the uplink Doppler in each receiver "on the fly". This article focused on the aspects of two-way ranging and Doppler but included a discussion of the problem of using a single uplink signal to multiple spacecraft. An analysis of the dynamics for this constellation involved a Doppler offset of 45 kHz and an uncompensated Doppler rate of 2.6 Hz/s, in which case signal acquisition performance was evaluated via SIMULINK.

For this study, we consider a more dynamic constellation consisting of lower-altitude orbiters such as those currently in orbit around Mars, where the frequency uncertainty regions (up to 200 kHz) and Doppler rates (up to 70 Hz/s) are higher. Although this constellation (shown in Figure 1) does not possess SDRs for the direct-to-Earth links, its mix of trajectories provides for a reasonable representation of Doppler offsets and Doppler rates to use for the study. The following section describes the Doppler dynamics for this constellation in detail.

III. Mars Geometry Example

The application of the MUPA technique we will consider involves the use of a single ground station tracking several spacecraft in orbit around and/or on or near the surface of Mars simultaneously. The MSPA technique is utilized for operational downlink. Figure 4 depicts a close-up of the geometry shown in Figure 1 where there are five spacecraft in orbit around Mars. For the purpose of clarification, although none of these spacecraft possess a usable SDR for the direct-to-Earth links, we will treat their collection of orbital parameters in our study to characterize the various Doppler rates and Doppler offsets that may be encountered in future scenarios involving spacecraft with SDRs

In Figure 4, the orbits for each spacecraft are shown as well as the locations of the spacecraft on October 7, 2016 at 23:25 UTC as seen from the Earth. For reference this scenario occurs at a range distance of 1.07 AU where Mars subtends an angle of 2.4 mdeg. Given that the 3 dB X-band beamwidth is 71 mdeg for a 34-m antenna, this translates to ~30 Mars diameters. Thus, when centered at Mars at a 1.07 AU distance, the uplink station's beam encompasses all of the Mars orbiting spacecraft.

Figures 5 and 6 depict the relative Doppler shifts between the possible 10 pairs of the five spacecraft for an approximate two month period spanning from September 30, 2016 to November 27, 2016. We see that the relative Doppler shift can reach magnitudes of as high as 165 kHz for the case of MRO and MAVEN. Table 1 displays the relative Doppler shift between pairs of spacecraft at Mars relative to an X-band uplink frequency of 7.15 GHz for the period spanning September 30, 2016 to November 27, 2016. For instance, over this two-month period, the minimum Doppler frequency would be 148.5 kHz for MOM versus the maximum of 336.56 kHz for MAVEN (both relative to the mean 250 kHz), resulting in an almost ±100 kHz Doppler offset relative to the mean Doppler over all five spacecraft.

These Doppler shifts can be different during other periods and during different phases of some of the missions (such as during orbit trimming), with values reaching up to 200 kHz covering a longer period of time. It should be kept in mind that the actual magnitudes of Doppler offsets and Doppler rates between spacecraft used for planning will depend upon utilizing the specific trajectory information over a shorter period of time, such as a one day period. This will usually result in smaller Doppler excursions than those encountered over the longer ~2 month period example previously discussed (see Figures 5-6).

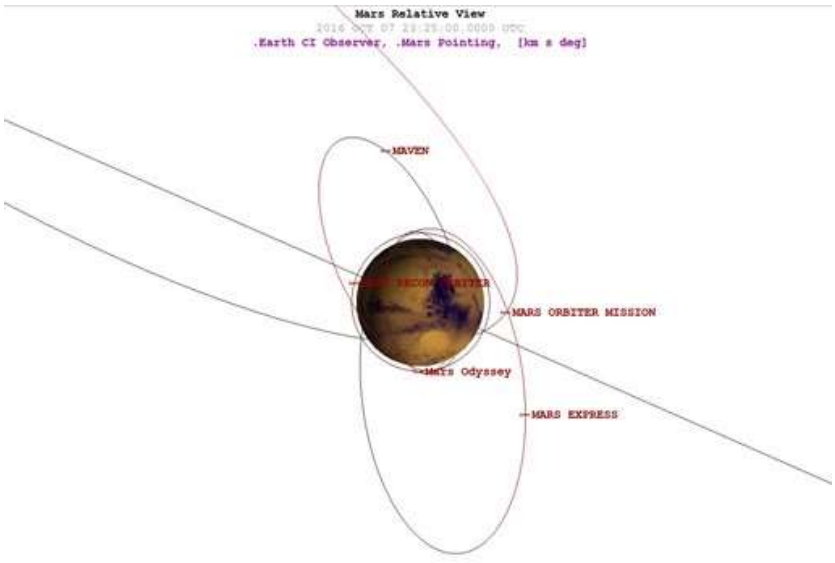

Figure 4 – SOAP[1] image showing geometry of Mars and its five orbiting spacecraft on October 7, 2016 at a range distance of 1.1 AU as seen from the Earth (close-up view of vicinity of Mars from Figure 1).

We expect the cases described here will provide a reasonable scenario for considering signal acquisition strategies for MUPA. Significantly different results would be obtained for constellations consisting of spacecraft orbiting in the same direction (lower relative Doppler effects) versus spacecraft with low altitudes orbiting in opposite directions (higher relative Doppler). Magnitudes of Doppler shifts and Doppler rates would be lower at the uplink frequency of 7.15 GHz relative to the 8.4 GHz downlink frequency. Two-way Doppler shift and rates would be approximately two times larger, but we consider the case of a one-way link from the Earth to the spacecraft such that the uplink is Doppler compensated to the center of Mars. Once each spacecraft acquires and locks onto the signal, a unique coherent turn-around frequency is then downlinked to the ground station for each spacecraft. The downlink for each spacecraft would then be processed by independent receivers which would themselves be Doppler compensated.

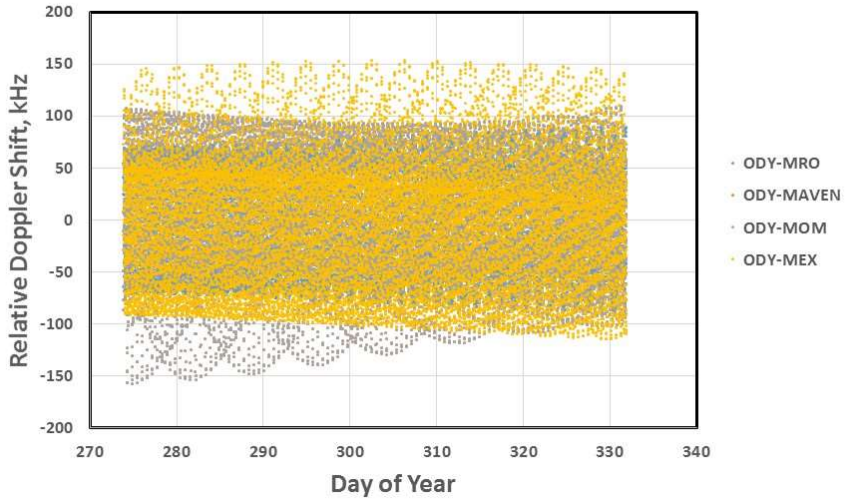

Figure 5 – Relative Doppler shift between pairs of spacecraft relative to 7.15 GHz uplink frequency from September 30, 2016 to November 27, 2016.

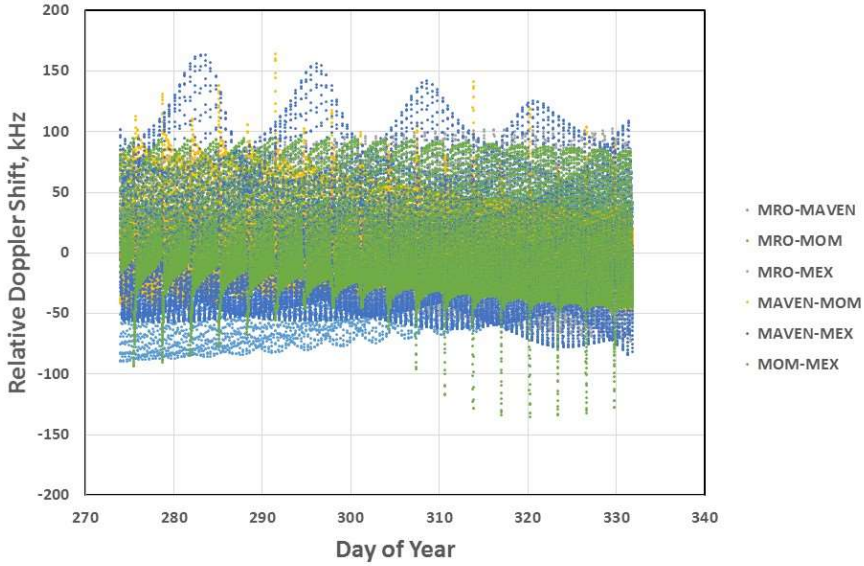

Figure 6 – Relative Doppler Shift between pairs of spacecraft relative to 7.15 GHz uplink frequency from September 30, 2016 to November 27, 2016.

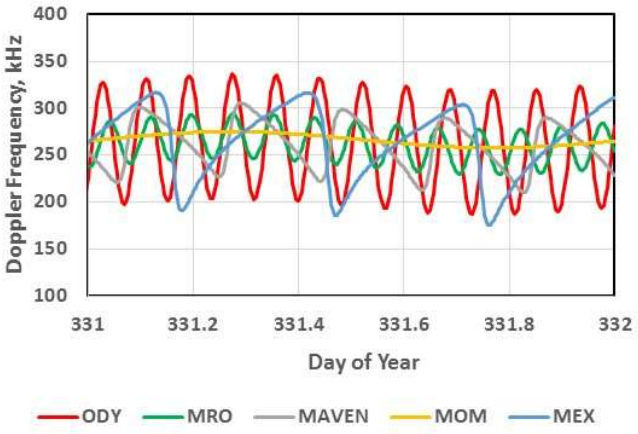

Figure 7 – Individual Doppler signatures for five orbiting Mars spacecraft during a one-day period on November 26, 2016 relative to an uplink frequency at 7.15 GHz.

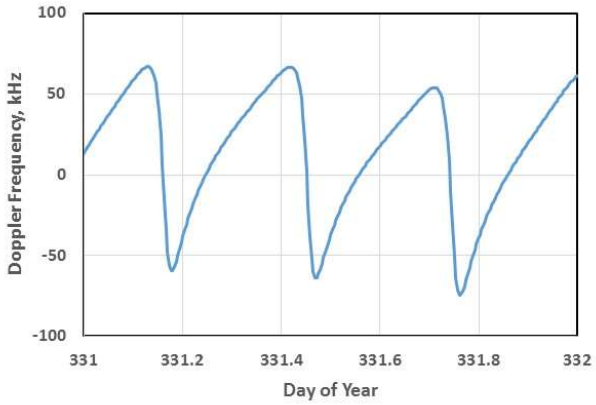

Figure 8 - Sample one day period of Doppler frequency for DSN to MEX relative to Mars centroid for uplink predicts (referred to 7.15 GHz)

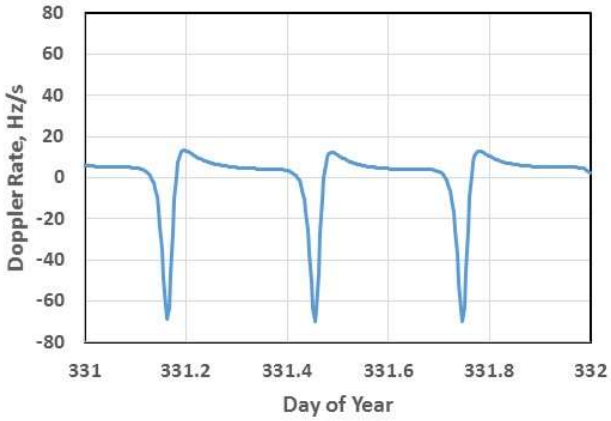

Figure 9 - Sample one day period of Doppler rate from Figure 8 Doppler.

For our signal processing analysis and for closer examination of the signatures, we choose to select the one day period on November 26, 2016. Figure 7 depicts the individual Doppler signatures for the five spacecraft during this one day period. A typical Doppler signature for the case of MEX relative to a DSN station for a 24-hour period is shown in Figure 8 (relative to a received 7.15 GHz signal). In this case, we assume that the uplink signal frequency is Doppler compensated with respect to the center of Mars. Figure 9 displays the Doppler rate (based on the Doppler

signature in Figure 8) for the same single day. Note that Doppler rates reach magnitudes as high as -70 Hz/s during this period.

Table 1

Relative Doppler Shifts between Spacecraft at Mars

X-band

Spacecraft Pair	Average (kHz)	Min (kHz)	Max (kHz)
ODY-MRO	-0.003	-90.6	89.2
ODY-MAVEN	-0.026	-158.0	108.8
ODY-MOM	-0.306	-88.6	154.1
ODY-MEX	0.025	-115.3	153.1
MRO-MAVEN	-0.023	-90.1	66.5
MRO-MOM	-0.303	-28.7	84.0
MRO-MEX	0.028	-73.4	102.3
MAVEN-MOM	-0.280	-54.8	163.2
MAVEN-MEX	0.051	-85.0	163.0
MOM-MEX	0.331	-135.9	94.3

IV. Signal Acquisition Algorithms

This section deals with signal search and acquisition algorithms that are needed for non-standard signal scenarios where the received frequency may lie significantly far away from the spacecraft receiver's NCO[e] best-locked frequency, as well as large uncompensated Doppler rates. Such algorithms include A) FFT signal search, B) step-and-sweep signal search and C) trajectory aided tuning.

A. Fast Fourier Transform (FFT)

The Fast Fourier Transform (FFT) signal search algorithm has been utilized by several entities (such as in GPS receivers) when there is a large frequency uncertainty window that is required to be searched in order to locate the signal prior to attempting to lock onto the signal. Such techniques require that the expected signal frequency lies somewhere inside the front-end search window of the receiver, which should be wide enough to accommodate all possible scenarios accounting for Doppler dynamics.

When there are high (uncompensated) dynamic conditions and relatively weak signal levels, the FFT algorithm may be plagued with issues of smearing and thus have difficulties achieving stable lock. Vilnrotter, Hinedi and Kumar[19] have evaluated several frequency estimation techniques for high dynamical conditions. They provided estimates of performance at low signal levels and high dynamics in order to determine the useful operating range of an approximate maximum likelihood estimator, an extended Kalman filter, a cross-product automatic frequency control loop, and a phase-locked loop. Numerical simulations were performed to evaluate performance while tracking a common trajectory exhibiting high dynamics. They concluded that the maximum likelihood approach attained the lowest loss-of-lock threshold (23 dB-Hz), as well as the lowest RMS estimation errors above threshold. The use of such techniques may be considered in future studies but are beyond the scope of this paper if one decides to go the FFT route.

We assume that only the carrier requires FFT acquisition for this study. For data modulated cases, the subcarrier and symbol frequencies or bit periods are well known such that FFT acquisition is not required for these once the carrier is detected. Thus, we are assuming only the case of residual carrier acquisition without any data modulation or ranging. Current deep-space radios such as UST and Iris have sufficiently wide front-end bandwidths and "acquisition/tuning" algorithms can be programmed into the flight software and firmware. For the purpose of this study, we chose to perform signal acquisition tests using the DSN gorund equipment and FFT signal search algorithm to gain insight into the technique, understanding that there may be some limitiations to generality of the test results.

[e] Numerically Controlled Oscillator

The DSN's ground receivers make use of the FFT signal search algorithm[20]. If one implements the DSN FFT search algorithm used to acquire the spacecraft signal at the ground on the spacecraft, we would use an algorithm similar to the following. Here the search band is partitioned into segments where FFTs are performed on each successive segment working its way iteratively away from the receiver's center tuned frequency. The FFTs are performed successively on segments centered around the nominal receiver center frequency. Once a signal is detected in an FFT segment, some additional processing is performed to avoid aliasing, and then some time is allowed for the PLLs to attempt, achieve and then report lock. We can think of the total signal acquisition time to be composed of two components; first, the time it takes for the signal to be detected and located in frequency in the FFT search, T_{FFT}, and, second, the time it takes for the loops to complete the locking process and report the LOCKED condition, T_{loop}. Thus, the total signal acquisition time is given by

$$T_{acq} = T_{FFT} + T_{loop} \qquad (1)$$

The time taken to perform the FFT search can be expressed as[20]

$$T_{FFT} = 2^M/fs \qquad (2)$$

where fs = section bandwidth, or sample frequency of FFT (ranges from 2 kHz up to 2000 kHz[20]) and where M is determined from a function of estimated signal strength (Pc/No), signal strength acceptance level criteria, and a zero pad factor for the FFT (defaulted to be unity for zero padding).

For weaker signals (small Pc/No), the number of data points per FFT grows to be large, hence the time for each FFT, T_{FFT}, becomes large relative to T_{loop} and will dominate acquisition time.

The time required for the loops to lock once their NCOs have been set[20] is conservatively estimated as:

$$T_{loop} = 20/B \qquad (3)$$

where B is the final tracking loop bandwidth. The added conservatism in Eq. 3 allows for the possibility that lock may not necessarily occur during the first lock detection period[20] and allows for additional time to achieve lock We expect that this contribution is a coarse estimate and the actual time it takes for the loops to be set is somewhat longer, but seldom reaches below 8-9 s lock-up times as was observed in our testing as well as in DSN operations.

We find that the signal acquisition time will vary between 10's of seconds to minutes depending upon SNR, loop bandwidths and other considerations. A maximum ±200 kHz frequency uncertainty range is based on an inferred maximum of estimates of relative Doppler of the spacecraft in orbit around Mars at X-band (see Section III).

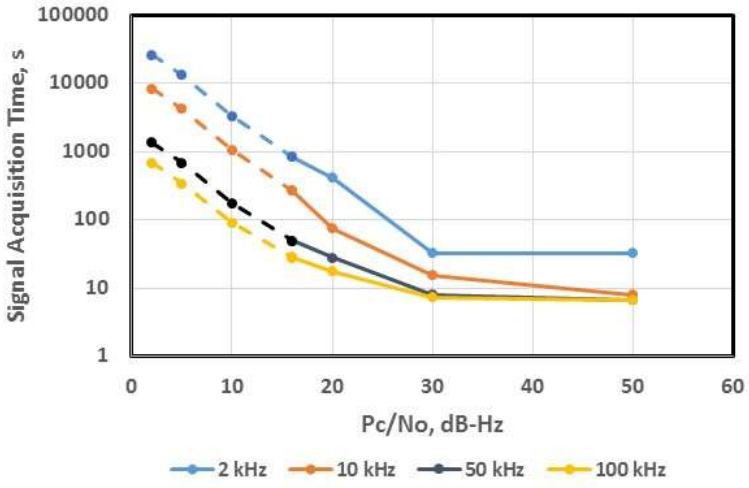

Figure 10 – Estimated signal acquisition times using DSN FFT signal acquisition algorithm where we assume the receiver is tuned to search around a frequency that is 100 kHz away from true received frequency. Above curves assume a 3 Hz final loop bandwith.

We now examine the signal acquisition times for a variety of different parameter values using the DSN FFT signal acquisition algorithm[20] summarized above. Figure 10 depicts the signal acquisition time as a function of incident

signal power to noise density (Pc/No) for four different FFT window sizes of 2, 10, 50 and 100 kHz when the incident frequency to the receiver is 100 kHz away from the tuned center frequency of the receiver. Figure 11 depicts the results for the case when the incident frequency is 200 kHz away from the tuned center frequency of the receiver. Note that for very large frequency uncertainty windows, the larger window sizes (50 kHz and 100 kHz) will tend to perform best (shorter signal acquisition times) than for smaller window sizes (2 kHz and 10 kHz). For the case when the signal strength is strong (Pc/No ≥ 30 dB-Hz), the signal acquisition times run about 10 – 20 s whereas for the weaker signals, the acquisition time can run from 10's to over 100's of seconds. It is cautioned that these are estimates only under relatively static conditions and do not consider effects due to Doppler dynamics, solar phase noise or transmitter phase noise. It should also be emphasized that points for the curves at lower Pc/No values in Figures 10 and 11 are dashed indicating that there is insufficient signal power to achieve or maintain lock for reasonable values of loop bandwidth, but they are provided for comparative purposes to allow inspection of the trends.

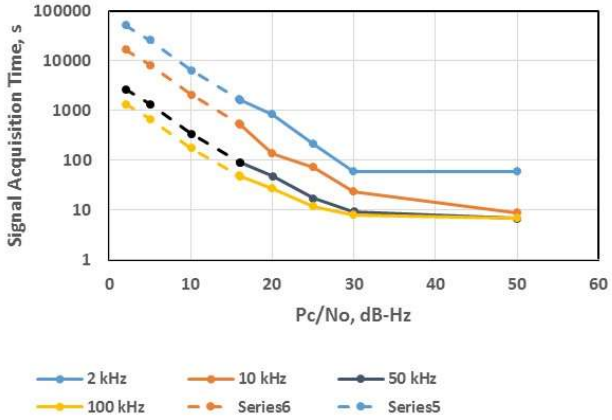

Figure 11 – Estimated signal acquisition times versus Pc/No using DSN FFT signal acquisition algorithm where we assume the receiver is tuned to search around a frequency that is 200 kHz away from true received frequency for different values of FFT bandwidth. Above curves assume a 3 Hz final loop bandwidth.

The DSN Test Facility (DTF-21) in Monrovia, California provides a testbed using duplicates of the same uplink and downlink equipment maintained at the three DSN sites in Goldstone, California, Madrid, Spain and Canberra, Australia (minus antennas and LNA front-ends) to allow testing of flight equipment or signal processing schemes. For the test reported here, the equipment set-up made use of an uplink signal generator, uplink-to-downlink frequency translator and receiver for coherent link testing and a signal generator and receiver for non-coherent link testing. The receiver was configured to perform the signal searching around a center expected received frequency, using the FFT search algorithm over large frequency uncertainty regions.

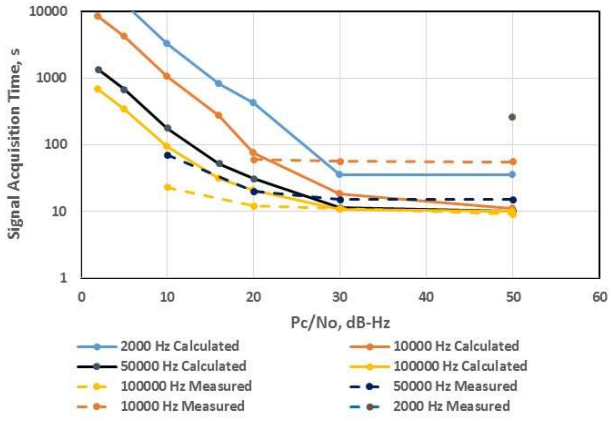

Figure 12 - June 27, 2017 Test with 100 kHz frequency uncertainty for FFT bandwidths noted in the legend. Calculated values from DSN algorithm and measured values from DTF-21.

We now discuss results of tests that were conducted at DTF-21. These tests were performed using a number of scenarios involving different loop types, acquisition and tracking bandwidths, Pc/No signal strengths, Doppler offsets and Doppler rates. These measurements of signal acquisition times were then compared with estimated signal acquisition times using the DSN FFT search algorithm[20] based on the same set of parameters.

Figures 12 and 13 depict the calculated and measured Tacq versus Pc/No for tests performed on June 27, 2017 at DTF-21. The points denoted by the dashed lines are from the measurements whereas the points connected by the solid lines are the predictions for the 100 kHz and 200 kHz frequency uncertainty regions, using the same parameter values as used in the tests. Although the dashed and solid line curves do not lie on top of each other for the respective frequency offsets, they are reasonable given the complexities and uncertainties of how the equipment behaves, as there are various checks performed by the equipment as well as some additional time lag between the actual lock-up time and the time that the lock-up is reported. Note that the largest descrepancies between calculated and measured signal acquisition times occur at the smaller FFT sizes.

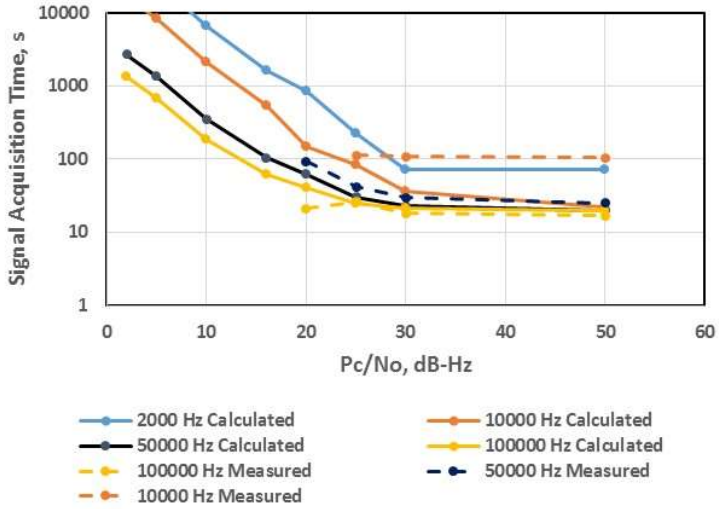

Figure 13 - June 27, 2017 Test with 200 kHz frequency uncertainty for FFT bandwidths noted in the legend. Calculated values from DSN algorithm and measured values from DTF-21 tests.

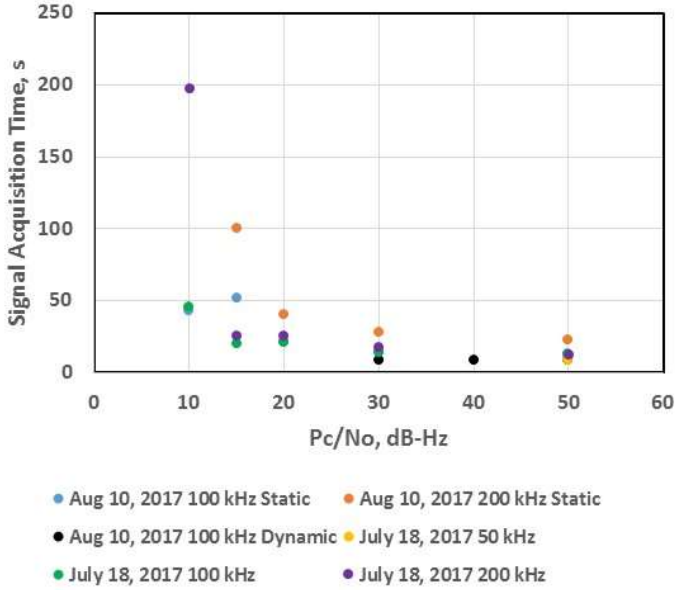

Figure 14 – DTF-21 July 18, 2017 Test Results for cases of 50 kHz, 100 kHz and 200 kHz frequency offsets, and August 10, 2017 test results for cases of 100 kHz and 200 kHz offsets. Note that there is overlap of some symbols.

A set of tests at DTF-21 conducted on July 18, 2017 and August 10, 2017 involved evaluating measured signal acquisition times for static frequency offsets (zero Doppler rate) of 50 kHz, 100 kHz and 200 kHz. Figure 14 depicts the measured signal acquisition time as a function of incident signal power-to-noise density (Pc/No) for frequency offsets of 50 kHz, 100 kHz and 200 kHz away from the tuned center frequency of the receiver for these tests. There is reasonable agreement with the predicted estimates. Note that the 100 kHz offset cases tend to acquire and lock more quickly than that of the 200 kHz offset as expected, and, as the signal strength decreases, the acquisition/lock-up times become greater as expected. In order to ensure sufficient loop SNR, small loop bandwidths were used at the lower signal power levels.

On August 10, 2017, we performed static tests at a frequency offset of 100 kHz (blue points in Figure 14), and a frequency offset of 200 kHz (orange points in Figure 14). Also performed were a set of dynamic tests (non-zero Doppler rate) at 100 kHz frequency offset (black points). The static test results were again consistent with previous static test results. The dynamic test results first attempt at 50 dB-Hz resulted in no lock with a 3 Hz initial loop bandwidth. When the final loop bandwidth was widened to 20 Hz, we got lock-up quickly at 9 seconds. At Pc/No = 40 dB-Hz, lock was again achieved using loop bandwidth settings of 20 Hz, with lock still being realized when the final loop bandwidth was narrowed to 3 Hz after the signal was acquired. We also achieved lock at 30 dB-Hz. Lower signal strength cases were tested but lock was not achieved suggesting that the signal was too weak for the given loop bandwidth given the dynamics. Attempting lock with future tests may possibly involve implementing frequency rate aiding of some type into the algorithms.

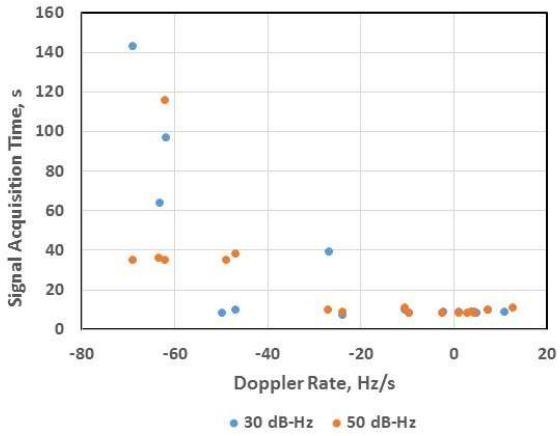

Figure 15 – Signal acquisition time as a function of Doppler rate.

Figure 15 documents the results of tests performed on November 16, 2017 where we characterize lock-up time as a function of uncompensated Doppler rate for signal strengths of 30 dB-Hz and 50 dB-Hz. Note that for magnitudes of Doppler rates of -40 Hz/s and smaller, lock up times generally run about 10 s for almost all cases. However, when Doppler rate magnitude exceeds -60 Hz/s, there is an increase in lock-up time with wider dispersion reaching values as high as ~140 s.

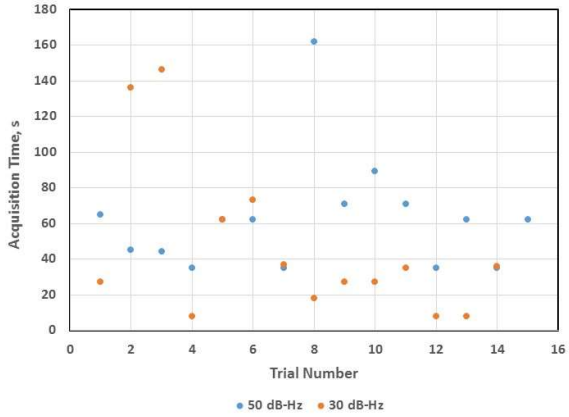

Figure 16 – November 21, 27-28, 2017 DTF-21 test results, lock up times as a function of trial number.

Figure 16 illustrates the dispersion in lock-up times for multiple runs at the same maximum Doppler rate of -68 Hz/s for 50 dB-Hz (blue) and 30 dB-Hz (orange) carrier-to-noise power density values. Here the horiziontal axis denotes the trial number of the acquisition attempt. We assume an FFT bandwidth of 500 kHz. It is noted that in several cases, the receiver did not lock up during the first series of FFT's within the frequency search range.

The purpose of using the DSN ground equipment to perform FFT signal acquisition tests was to get a sense of the various ideosynchronsies that could be encountered with this algorithm when applied to a spacecraft. The use of this algorithm aboard spacecraft with SDR's would involve programming in the firmware to perform the signal processing needed to locate the frequency of the signal. Such processing would include interaction with the flight software. Once established, the detected frequency would be used to tune the NCO in which to perform the standard acquisition technique to enable lock-up. For cases of high Doppler rates (high frequency dynamics), a sequence of FFTs could be performed in which to establish a Doppler rate that could be used in aiding with the detected Doppler frequency sent to the NCO. One such method that has been discussed involving high dynamic situations (such as with GPS) was a method used to track signals on spacecraft undergoing severe maneuvers normally performed with aiding from an inertial navigation unit (INU) on the receiver. In lieu of this method, a new concept that enables high dynamic tracking without depending on the INU involves such an approach using FFT for frequency estimation and a maximum likelihood estimator for delay[21].

Bell et al.[22] discuss potential multi-user receiver architectures for SDRs such as for the case of a Mars orbiter simultaneously supporting multiple surface assets. Such FFT-based acquisition approaches discussed here may prove applicable for MUPA. Satorius et al.[23] discussed potential FFT signal search performance for direct-to-Earth EDL for the Mars Exploration Rover spacecraft, which included frequency rate search during carrier acquisition under high dynamic conditions.

B. Step-and-Sweep Signal Search

A second carrier signal acquisition technique makes use of the step-and-sweep algorithm, where the frequency uncertainty range is partitioned into successive discrete overlapping search bands. The NCO is successively tuned to the middle of each band, and the radio performs a signal search within each carrier loop acquisition bandwidth, starting from one end of the frequency search bandwidth to the other end. If insufficient energy is encountered in one search region, the algorithm steps into the next search bandwidth, with some overlap. Once a signal of sufficient energy is found, the alogorithm may continue to search adjacent bands until the band with maximum signal amplitude is identified. The NCO is then tuned to this frequency and the loop then attempts lock. This design was implemented on the Electra radio and used by several projects in proximity links between landed assets on Mars and orbiters equipped with an Electra radio such as MRO[24]. The Electra radio provides communications and navigation services for Mars mission proximity links. This radio flew for the first time on MRO and, as of the date of publication, is still operating. The MAVEN orbiter and ExoMars Trace Gas Orbiter both use Electra radios. A future spacecraft that will carry Electra is the Mars 2020 Rover. The MSL Curiosity rover makes use of a lite version of Electra[25] when it communicates with one of the orbiting assets.

The acquisition algorithm used by Electra is open-loop and usually predict-based. This radio employs a digital approach where the incoming waveform is downconverted to baseband and the in-phase (I) and quadrature (Q) components are digitally generated, sampled and processed. The acquisition/tracking loop is a second order PLL with a loop bandwidth that ranges from 10 Hz to 10 kHz. The radio has a required tracking range of ±20 kHz, and a required tracking rate of ±200 Hz/s[26], which can easily accommodate a Doppler rate of ~70 Hz/s for the Mars constellation being considered for this study (see Section III). The Electra radio scans the frequency uncertainty region about the expected received center frequency using a step-wise sweep, half pull-in band over a 50 kHz to 200 kHz window. The step-and-sweep algorithm is described in detail elsewhere[26-27].

A series of initial tests were conducted in 2004 prior to MRO's launch involving the MRO Engineering Model (EM) and Flight Model (FM) Electra units in order to determine carrier acquisition speed under various operating modes and loop SNR conditions[6]. These tests involved generating carrier and telemetry signals as input to the Electra units under test. Signal strengths were maintained with a carrier loop SNR of about 14 to 15 dB. The test signal frequency was purposely offset from the center receive frequency to test lock-up times over wide frequency uncertainty regions and Doppler rates. Some tests involve zero Doppler rates (static) while others involved non-zero Doppler rates[6] (dynamic). However, tests involving the Electra testbed were only performed with frequency offsets of up to ~40 kHz, which was sufficient for the expected Doppler uncertainty due to the proximity geometry at the low UHF frequencies utilized by the radio (~401-435 MHz) expected to be encountered by MRO during relay operations.

Predicted signal acquisition times using the documented signal acquisition time algorithm[24] for Electra are provided in Figures 17 and 18. Figure 17 displays carrier acquisition times for given symbol rate settings and Es/No settings for a frequency search window of 100 kHz where the input signal frequency is intentially set 100 kHz away from the nominal receiver frequency, and Figure 18 displays the signal acquisition times for a frequency search window of 24 kHz. Here we assume the entire frequency uncertainty window is searched in steps of carrier loop bandwidth starting from one end with the signal residing at the end of the window. A couple points must be kept in mind. First, the signal acquisition algorithm pertains to only carrier acquisition. No attempt is made to lock onto the telemetry as the symbol rates and symbol energy-to-noise ratios, Es/No, are only configurable settings in the radio that determine the quantities of the search algorithm such as carrier loop bandwidths, decimation factors, clock sample rates, and dwell times. As the symbol rate setting is increased, this allows for accommodating increased received power, so that we have increased carrier loop acquisition bandwidth to allow the same loop-SNR to be maintained for the given scenario until the maximum permitted carrier loop bandwidth value of 10 kHz is reached. The results of Figures 17-18 convey that carrier acquisition/lock times range from ~1 ms to ~1 s over most possible scenarios provided that adequate signal power is available.

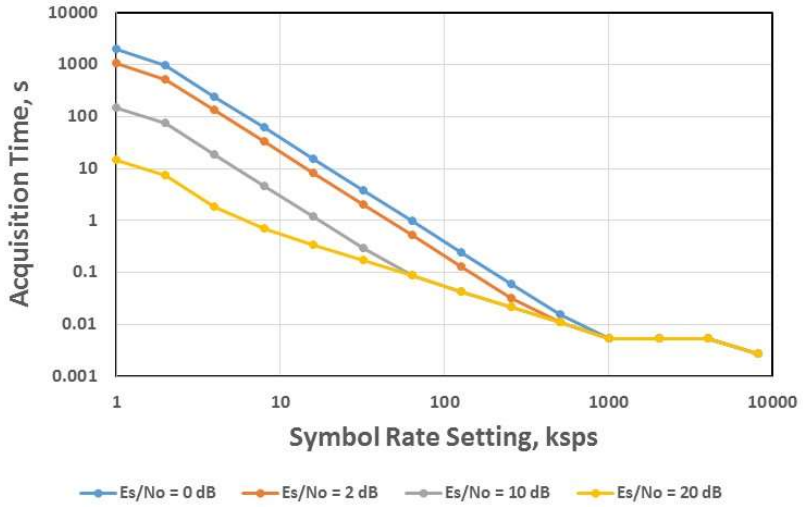

Figure 17 – Predicted carrier acquisition times for given symbol rate settings and Es/No settings for a frequency search window of 100 kHz.

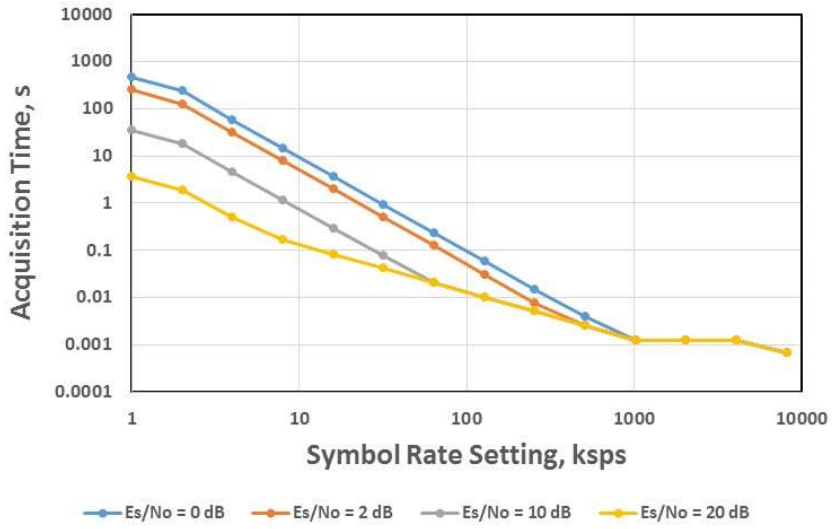

Figure 18 - Predicted carrier acquisition times for given symbol rate settings and Es/No settings for a frequency search window of 24 kHz.

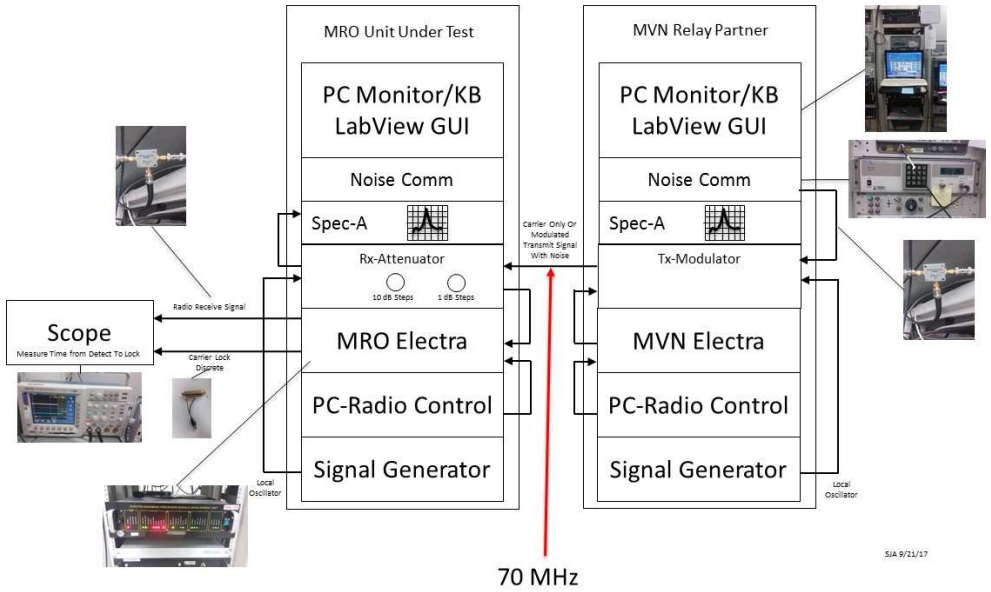

Figure 19 – Test set-up for 2017 tests - left rack includes MRO Electra EM and associated equipment used to receive the signal (at an IF of 70 MHz) - the right rack includes the MAVEN (MVN) EM and associated equipment used to generate the test signal.

A series of tests were performed in 2017 involving the Electra testbeds residing at JPL which included EMs of the MRO and MAVEN Electra radios (see Figure 19). These tests exercised the Electra signal search algorithms for frequency uncertainty regions of up to 50 kHz. The recent tests used the setup depicted in Figure 19 where the MRO EM served as the receiver and the Electra Maven relay partner testbed served as the signal source. Additional supporting hardware is also shown in the block diagram along with photos of selected equipment. The Rx-attenuator served to set the signal level at the receiver input to the Electra receiver at appropriate levels.

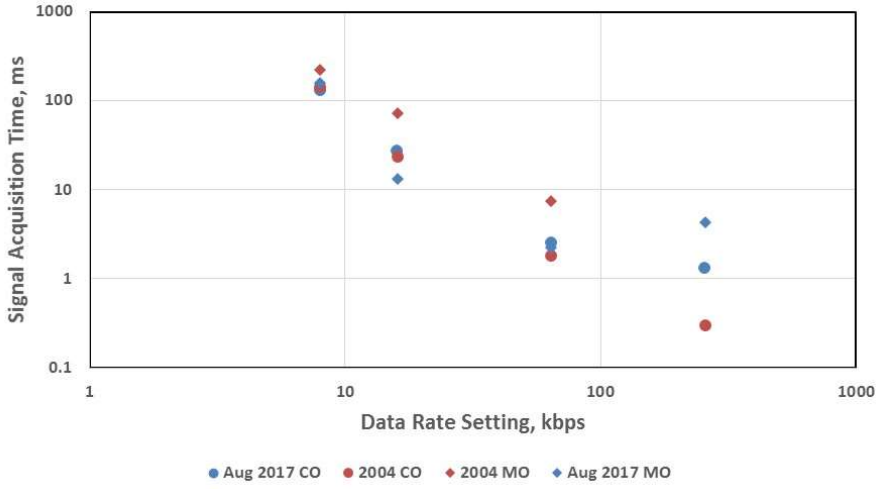

Figure 20 – Carrier only (CO) signal acquisition times for a series of tests conducted on August 29, 2017 (blue circles) along with corresponding results from 2004[6] (red circles) with modulation turned off. Carrier signal acquisition times with modulation turned on (MO) were performed for a series of tests conducted on August 2017 (blue diamonds) along with corresponding results from 2004 (red diamonds). There may be overlap of some symbols.

The new series of tests were performed in 2017 to yield signal acquisition and lock times for certain cases similar to what was done in 2004 in order to check the consistency of the current test set-up with that used in 2004. The mean, minimum and maximum statistics of lock times were estimated. Figure 20 depicts the average carrier acquisition time values for the recent tests conducted in August 29, 2017 for the cases of carrier-only (CO with modulation turned off) (blue circles), carrier acquisition with modulation turned on (MO) (blue diamonds), along with the results of the 2004

tests for carrier-only (CO) (blue circles) and for carrier with modulation turned on (MO). The tests involved an Es/No setting of 10 dB resulting in different acquisition times for frequency offsets of up to 24000 Hz with an acquisition search bandwidth of 24000 Hz.

The average acquisition times for the 2004 tests given in Figure 20 (filled orange circles) and 2017 tests (filled blue circles) involving carrier-only (CO) were in reasonable agreement for the most part, decreasing with increased data rate setting, thus providing a reasonable sanity check. The minimum and maximum acquisition times from these tests (not shown) were also in reasonable agreement with those from the earlier 2004 results[6]. Only at the highest data rate setting case was the difference significant. In addition, the 2004 tests involved random frequency offsets of up to 24000 Hz while the 2017 tests involve a full 24000 Hz offset for each of the multiple runs. In all cases, the acquisition times were well below a second.

A series of acquisition runs were also performed with modulation enabled (MO) and the mean, minimum and maxium statistics were estimated using an acquisition search bandwidth of 40000 Hz. Figure 20 depicts the average acquisition time values for the 2017 tests involving modulation enabled (MO) (blue diamonds) and the average values from the 2004 tests involving modulation enabled (MO) (orange diamonds). As one can see, the average acquisition times were in agreement within an order of magnitude for the most part, but decreasing with increased data rate. Here we see that the recent tests had lower signal acquisition times than those of the earlier 2004 tests. The minimum and maximum acquisition times from the recent runs were also in reasonable agreement with those from the earlier 2004 runs. In all cases, the signal acquisition time was significantly less than one second.

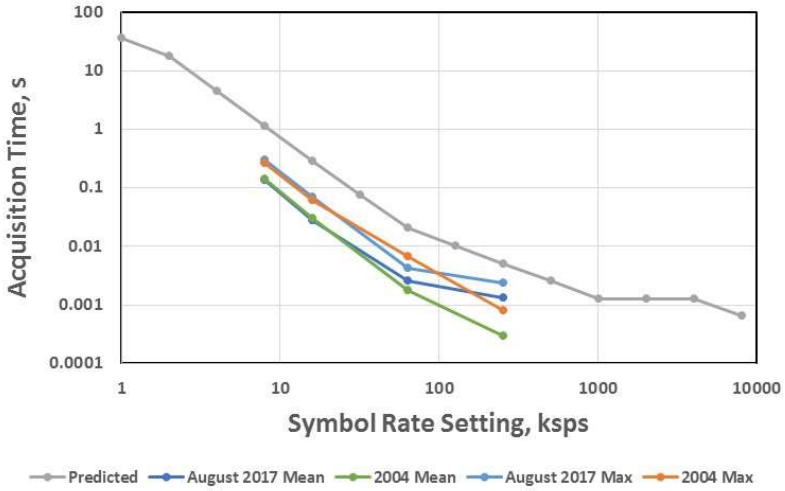

Figure 21 – Predicted acquisition times (grey) compared against 2004 and 2017 measured mean and max acquisition times for carrier-only case with frequency offset of 24 kHz.

Figure 21 depicts the predicted acquisition times using the documented algorithm[6,24] (grey) with the assumption that the entire 24 kHz band is searched before encountering the signal, along with mean and maximum acquisition times calculated from measurements of multiple runs with random Doppler offsets and rates for the case of carrier-only. The measured acquisition times (colored points) are basically quicker than the predicted times (gray points), and this is consistent with the observation made by the 2004 testers that the Electra sometimes "grabs" the signal early-on while not all of the steps are being completed[6]. This also depends on where in the algorithm the center frequency and other parameters are selected.

Figure 22 depicts the predicted acquisition times using the same algorithm[6,24] (gray), but this time assuming an entire 40 kHz band is searched before finding the signal. Also shown are mean and maximum acquisition times calculated from measurements from multiple test runs with random Doppler offsets and rates for the case of carrier-only with modulation turned on. Again, we see that the measured acquisition times are basically quicker than the predicted times, consistent with the above stated observation made by the early testers[6]. This also depends on where in the algorithm the center frequency and other parameters are selected. Thus, the predicted grey curves in Figures 21 and 22 serve as a reasonable upper bounds to the measurement sets.

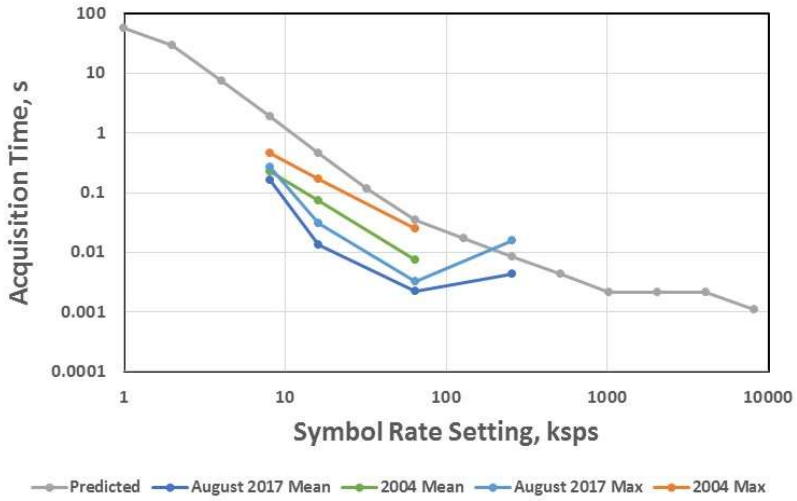

Figure 22 – Predicted carrier acquisition times (grey) compared against testbed measured acquisition times for modulation-enabled case with frequency offset of 40 kHz

Figure 23 displays carrier acquisition lock times over multiple runs for several cases of loop SNR during static signal conditions (constant Doppler frequency input). Here we see that lock easy occurs within 50 ms for all cases of loop SNR. The largest frequency offset of 99 kHz (green points) results in higher acquisition times as expected over the smaller frequency offsets of 31 kHz and 49 kHz.

Referring back to Figure 17, for a 100 kHz frequency offset search region, one sees that for a Es/No setting of 10 dB, we can achieve lock well within a second for all symbol rates from 8 ksps to well above 1 Msps using the Electra step-and-sweep algorithm. It should be kept in mind that the symbol rate and Es/No values pertain only the Electra radio settings which determine the signal acquisition approach, and are not the actual values that may be included in a link budget scenario, since no attempt was made to lock onto the telemetry channel. However, the carrier is usually very quick to achieve lock, and the full-lock state including symbol lock should easily be realized shortly thereafter. Reasonable values of signal acquisition time are achieved using this algorithm which holds promise for quick searches in SDRs when there are large frequency offsets and high Doppler rates. Porting this architecture to spacecraft replacing the analog type radios (e.g., SDST) holds a lot of promise for performing quick signal acquisitions assuming adequate signal strength, etc.

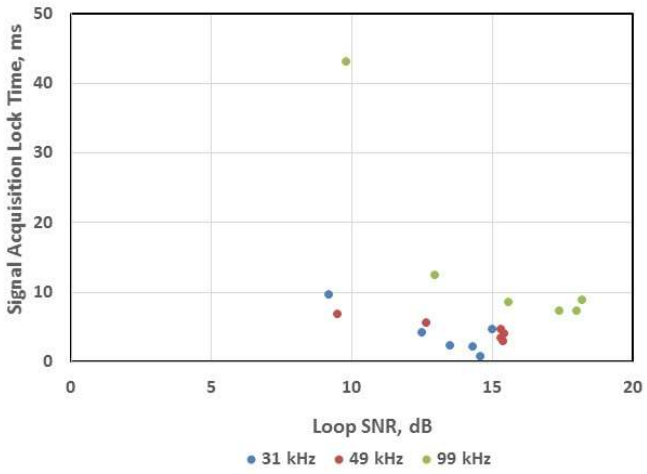

Figure 23 – Average carrier acquisition lock times over multiple runs for several cases of loop SNR.

The above results provide discussion of predictions and measurements of acquisition times over a limited range of frequency offsets and Doppler rates. The SIMULINK tool[17] was tuned to allow for estimation of signal acquisition

times for a wider range of offsets and rates for several step-and-sweep search scenarios[f]. Initial results for frequency offsets of up to 100 kHz and a Doppler rate of -70 Hz/s, yielded acquisition times ranging from ~0.5 s at very high SNR to ~ 6.6 s for a reasonably strong loop-SNR of 30 dB. A more comprehensive report of these simulations will be focus of a future study, including results for Doppler rates of up to 200 Hz/s.

In order to supplement the above results, we also examined early test results involving the MCAS receiver[28] which was a precursor to Electra, but involved a similar architecture. Average lock times for no Doppler offset and zero Doppler rate ran well below 1 s over a wide range of symbol SNRs and data rates. When Doppler offsets were added to the carrier, the acquisition times increased significantly as expected. For low data rates, the acquisition times ran ~10 s at low Eb/No settings and decreased to less than 4 s at high Eb/No settings. In all cases, the average time to lock was less than the time required to perform one complete sweep. For the cases of the highest data rates with Doppler offsets, the acquisition times were less than 20 ms over all Eb/No settings, with the trend showing a decrease in acquisition time as Eb/No setting increased. As part of the MCAS testing, the maximum Doppler rates for stable tracking were determined, which ran from 2500 Hz/s for 4096 ksps symbol rate over all Eb/No settings, to just less than 115 Hz/s at 1 ksps[28]. The MCAS testing showed overall quick acquisition times using their sweep method. We expect appropriate step-and-sweep radio designs to perform similarly or better, pending potential future studies involving testbed implementation and testing.

V. Trajectory-based On-Board Tuning of Spacecraft Radio

One can also deal with large frequency uncertainty regions caused by the desire to send a single uplink signal to multiple spacecraft by performing on-board frequency tuning. This can be accomplished by periodically uplinking appropriate trajectory/ephemeris information to the spacecraft along with knowledge of the location of the uplink station. The on-board software can either perform the appropriate estimation process to yield the expected Doppler frequency as a function of time, or make use of an uplinked look-up table of expected Doppler frequencies for given passes. When the spacecraft is nearing a tracking pass, the flight software will send an estimate of the frequency to the digital processing firmware to steer the NCO close to the expected uplink frequency where it can then perform a standard acquisition. For cases where there are short periods of time between passes, the flight software can be programmed to send instructions to the firmware to change filter coefficients with short time constants to zero out the phase error and reset the NCO to its nominal frequency in preparation for the next pass.

This technique was explored by Johns Hopkins University Applied Physics Lab (JHU/APL) and is planned for use in a future proximity link involving the Frontier radio which was developed primarily for deep-space applications[29]. The Frontier Radio is an SDR designed for spaceborne communications, navigation, radio science, and sensor applications. An S-band version of this radio was used on the Van Allen Probes mission[12] thus providing flight heritage in the near-Earth space domain. Dual-band X/Ka versions of this radio are being developed for the Parker Solar Probe and Europa Clipper missions. This radio will be used by Parker Solar Probe[13-15], which is planned for a 2018 launch. The radio uses software and firmware to allow enhancement of its digital signal processing capabilities.

Some signal acquisition/lock testing was performed for the radio planned for use by the Parker Solar Probe[11,13]. Two cases involving a large Doppler offset and a small Doppler offset were considered. The cases discussed here were generated for an Eb/No = 11.5 dB with a 7.8125 bps uplink command rate. At a 90% cumulative probability, the large Doppler offset case had an acquisition time of about 26 s whereas the small Doppler offset condition had an acquisition time of about 10 s. This study was conducted to test robustness and acquisition of the symbol tracking loop in low SNR conditions with different command rates and different Doppler offset conditions[13]. The 90 percentile lock-up times ranged from 40 ms at the highest data rate conditions (2 Mbps) to 26 s at the lowest data rate conditions (7.8125 bps). Carrier lock usually occurred quickly, and was not significant relative to that of the subcarrier and symbol loops, and thus was not addressed in the APL papers.

The Parker Solar Probe and Europa missions do not plan to make use of any non-standard acquisition strategies for direct-to-earth (DTE) communications as they will rely on the DSN to provide uplink frequencies that are tuned to near the expected received frequency of the radio which will perform standard acquisition. However, the Europa Clipper mission does plan to make use of non-standard digital signal detection techniques for the relay function between the Clipper spacecraft and lander. A technique is employed whereby the receiver accepts a Doppler prediction frequency to shift the carrier acquisition loop by a fixed offset in frequency to aid in acquisition and lock[29]. It is also planned that the Clipper spacecraft will monitor the lander signal over a wide bandwidth, record the signal data in open-loop mode and then send the data to Earth via the DTE link for further processing and analysis.

[f] Dariush Divsalar, Jet Propulsion Laboratory, Pasadena, California, private communication, April 12, 2018.

It should be noted that the current design of the Frontier radio is not an SDR in the strict sense, as that usually implies it would be re-programmable after launch. The Frontier radio software and firmware cannot be changed once it is set, and thus is not re-programmable after launch. A future design of the Frontier Radio FPGA, though, could be reprogrammable, which may allow for advanced FFT signal acquisition.

VI. Future Work and Conclusions

Several different radios are continuing to be explored to investigate the feasibility of using signal acquisition algorithms such as step-and-sweep and FFT searches, as well as making use of uplinking trajectory information to allow on-board frequency tuning using predicts generated from the ground station and spacecraft's state vectors or from time-tagged Doppler frequency look-up tables. Some potential testbeds or radios that could be utilized for further testing, include the Electra, Iris, CoNNeCT, UST and ML-605. These testbeds (or any available engineering models) could be used to exercise various signal search/acquisition algorithms for Doppler offset and rate operations such as what might be expected with MUPA for planetary orbiter constellations or small sat constellations.

The product of the loop update time, T_u, of the radio and the acquisition bandwidth, B_L, should be small, lying at or below 0.05 in order to allow for adequate loop performance thus enabling an essentially constant steady-state phase error, since loop performance degrades at higher T_uB_L products[30]. We see that this criteria is satisfied for several of the radios given their provided parameters (e.g., clock speed, loop update time).

The DSN receiver (whose testing results were discussed in Section IV.A) is limited by an update time such that with the bandwidth-time product constraint of 0.05, its highest value of acquisition bandwidth that can be accommodated is 100 Hz (versus 10 kHz for Electra). However, virtually all DSN missions make use of accurate trajectory compensation such that standard operations do not require higher acquisition bandwidths. Thus, if needed, the DSN FFT search algorithm can be initiated to search for the signal frequency within a much higher FFT bandwidth which then provides this information to the phase-locked loops.

Initial indications are that SDRs can easily accommodate on-board frequency tuning assuming that trajectory information is available on the spacecraft along with a ground station support schedule covering several tracking passes. Appropriate software needs to be programmed on the spacecraft computer to allow periodic tuning of the PLL NCO in the radio firmware. In lieu of on-board trajectory-based frequency tuning, the spacecraft SDRs can perform signal search and acquisition using the step-and-sweep algorithm or an FFT-based algorithm. The step-and-sweep algorithm such as used by the Electra radio has been successful and holds much promise. This algorithm can be easily implemented on several current SDR designs used for deep-space communications as provision is already available to allow NCO tuning from the spacecraft computer to the radio firmware, with minimal refinement to the firmware. In this case, the algorithm on-board the spacecraft computer would likely make use of a frequency uncertainty range and a search algorithm involving various step parameters (bandwidths, dwell times, etc.), given knowledge of the trajectory information of the rest of a constellation. An usable FFT search algorithm would require additional modifications to firmware and judicious exchange of information, such as commanding and processing between radio and computer. FFT searches are routinely performed by GPS receivers, and may be beneficial for future designs of deep-space radio firmware and on-board computer software algorithms. In any event, signal acquisition performance will be dependent upon the radio capabilities involving loop update time (or clock speed) and bandwidth as well as receiver sensitivity (higher SNR).

The testing of the various flavors of step-and-sweep and FFT-based signal acquisition schemes can thus be continued using available radios (or testbeds). This would require appropriate signal processing code to be implemented in the flight software and FPGA firmware. Such algorithms, including trajectory aided tuning, can be developed and tested to provide for reasonable radio designs for future missions where MUPA may be utilized, such as in small-SAT constellations or a future Mars orbiting fleet utilizing SDRs. Such future studies would include a quanitative comparison of lock times or probability of lock based on the exercise of the various signal acquisition schemes for a given radio.

Acknowledgments

We would like to thank Julian Breidenthal and Edgar Satorius of JPL for well appreciated review comments and suggestions; Ricardo Chincha of Peraton, Monrovia for providing valuable assistance in helping to set up and conduct many of the tests at DTF-21; Steven Allen of JPL for his help in setting up and conducting the tests involving the Electra test lab; D. Bell, J. Lux, C. Duncan, L. Torgerson, S. Clancy, K. Cheung, and D. Divsalar of JPL for much appreciated advice and support; David Copeland and his colleagues at JHU/APL for many informative discussions on the Frontier radio; and Wallace Tai for his sponsorship of this paper. The research was supported by NASA's Space

Communications and Navigation (SCaN) program. The research was carried out at the Jet Propulsion Laboratory, California Institute of Technology, under a contract with the National Aeronautics and Space Administration.

References

[1] Stodden, D. Y. and Galasso, G. D., "Space System Visualization and Analysis Using the Satellite Orbit Analysis Program (SOAP)," *Proceedings of the 1995 IEEE Aerospace Applications Conference*, Aspen, Colorado, February 4–11, 1995.

[2]Abraham, D. S., Finley, S. G., Heckman, D. P., Lay, N. E., Lush, C. M., and MacNeal, B. E., "Opportunistic MSPA Demonstration #1: Final Report," InterPlanetary Network Progress Report 42-200, pp. 1-27, Jet Propulsion Laboratory, Pasadena, California, February 15, 2015.

[3]Mysoor, N. R., Perret, J. D., and Kermode, A. W., "An X-band spacecraft transponder for deep space applications-design concepts and breadboard performance," in IEEE Transactions on Microwave Theory and Techniques, vol. 40, no. 6, pp. 1192-1198, Jun 1992. doi: 10.1109/22.141351

[4]Pugh, M., Kuperman, I., Aguirre, F., Mojaradi, H., Spurgers, C., Kobayashi, M., Satorius, E., and Jedrey, T. "The Universal Space Transponder: A Next Generation Software Defined Radio", *IEEE Aerosp. Conf.*, Big Sky, Montana, March 2017, 978-1-5090-1613-6/17//$31.00 ©2017 IEEE 1.

[5]Edwards, C. D., Jedrey, T. C., Schwartzbaum, E., and Devereaux, A. S., DePaula, R., Dapore, M., and Fischer, T. W., "The Electra Proximity Link Payload for Mars Relay Telecommunications and Navigation", *54th International Astronautical Congress of the International Astronautical Federation, the International Academy of Astronautics, and the International Institute of Space Law*, 29 September - 3 October 2003, Bremen, Germany.

[6]Bell, D., Racho, C., and Arnold, B., "Electra Acquisition Tests, Draft Version", Internal Report, Jet Propulsion Laboratory, Pasadena, California, October 25, 2004.

[7]Sutton, P. D. et al., "Iris: an architecture for cognitive radio networking testbeds," in *IEEE Communications Magazine*, vol. 48, no. 9, pp. 114-122, Sept. 2010. doi: 10.1109/MCOM.2010.5560595

[8]"ML605 Hardware User Guide", UG534 (v1.8) October 2, 2012, Xilinx Inc., https://www.xilinx.com/

[9]Reinhart, R. C., and Lux, J. P., "Space-based Reconfigurable Software Defined Radio Test Bed aboard International Space Station", *Space Ops Conferences*, 5-9 May 2014, Pasadena, CA SpaceOps 2014 Conference.

[10]Johnson, S. K., Reinhart, R. C., and Kacpura, T. J., "CoNNeCT's approach for the development of three Software Defined Radios for space application," *2012 IEEE Aerospace Conference*, Big Sky, MT, 2012, pp. 1-13. doi: 10.1109/AERO.2012.6187147

[11]Xie, H., Dolinar, S., Chase, M., Clancy, S., Kilzer, M., and Torgerson, L., "Flight test and validation of Variable Coded Modulation Using SCaN Testbed", Interplanetary Network Progress Reports, 42-212, Jet Propulsion Laboratory, Pasadena, Calif., February 15, 2018

[12]Crowne, M. J., Srinivasan, D., Royster, D., Weaver, G., Matlin, D., and Mosavi, N., "Spacecraft-level verification of the Van Allen Probes' RF communication system," *2013 IEEE Aerospace Conference*, Big Sky, MT, 2013, pp. 1-13. doi: 10.1109/AERO.2013.6497149

[13]Kufahl, K., Adams, N., and Kirschner, W., "Data Acquisition Performance for Deep Space Communications in Solar Probe Plus Frontier Radio", *2016 IEEE Aerosp. Conf.*, Big Sky, MT, 978-1-4673-7676-1/16/$31.00c 2016 IEEE

[14]Haskins, C. B., Angert, M. P., Sheehi, E. J., Millard, W. P., Adams, N., and Hennawy, J. R., "The Frontier Software-Defined Radio for the Solar Probe Plus Mission", *2016 IEEE Aerospace Conference*, Big Sky, MT, 2016, pp. 1-11. doi: 10.1109/AERO.2016.7500770

[15]Kufahl, K., Wortman, K., Burke, L., Hennawy, J., Adams, N., and Sheehi, J., "Flight Software Verification Methods in Frontier Radio for Solar Probe Plus Mission", 978-1-5090-1613-6/17/31.00c 2017 IEEE.

[16]Redbook, National Telecommunications and Information Administration, United States Dept. of Commerce https://www.ntia.doc.gov/files/ntia/publications/redbook/2012-05/5_12.pdf.

[17]Cheung, K., Divsalar, D, and Bryant, S., "Two-Way Ranging and Doppler for Multiple orbiting Spacecraft at Mars", 2018 IEEE Aerosp. Conf., 978-1-5386-2014-4/18/$31.00 ©2018 IEEE

[18]Cornish, T., "Single-Aperture Multiple-Carrier Uplink Using a 20 Kilowatt X-Band Transmitter," Telecommunications and Mission Operations Progress Report, 42-144, Jet Propulsion Laboratory, Pasadena, Calif., October-December 2000, pp. 1-20, February 15, 2001.

[19]Vilnrotter, V. A., Hinedi, S., and Kumar, R., "Frequency Estimation Techniques for high Dynamic Trajectories", *IEEE Trans. on Aero. and Elect. Sys.*, Vol. 25, No. 4 July 1989

[20]Kinman, P., "34-m and 70-m Telemetry Reception," DSN Telecommunications Link Design Handbook , DSN No. 810-005, Space Link Interfaces, Module 207, Rev. H, Jet Propulsion Laboratory, Pasadena, California, March 5, 2015. https://deepspace.jpl.nasa.gov/dsndocs/810-005/207/207A.pdf

[21]Hurd, W. J., Statman, J. I., and Vilnrotter, V. A., "High Dynamic GPS Receiver Using maximum Likelihood estimation and Frequency Tracking", *IEEE Trans. on Aerosp. and Electron. Sys*., VOL. AES-23, NO. 4 JULY 1987 425

[22]Bell, D., Satorius, E., Kuperman, I., and Koenig, J., "Multiuser Receiver Architectures for Space Modems," Interplanetary Network Progress Report, Jet Propulsion Laboratory, Pasadena, Calif., 42-198, pp. 1-13, August 15, 2014.

[23]Satorius, E., Estabrook, P., Wilson, J., and Fort, D., "Direct-to-Earth Communications and Signal Processing for Mars Exploration Rover Entry, Descent, and Landing," Interplanetary Network Progress Report, Jet Propulsion Laboratory, Pasadena, Calif., 42-153, January-March 2003, pp. 1-35, May 15, 2003.

[24]Bell, D., Taylor, J., and Devereaux, A., “Mars Reconnaissance Orbiter, UHF Telecommunications System Operations Handbook”, Revision B, June 20, 2012, JPL D-34870, MRO-58-790, Jet Propulsion Laboratory, Pasadena California 91009.

[25]Bell, D., et al., "MRO relay telecom support of Mars Science Laboratory surface operations," *2014 IEEE Aerospace Conference*, Big Sky, MT, 2014, pp. 1-10. doi: 10.1109/AERO.2014.6836170

[26]Lee, D., “Mars Reconnaissance Orbiter Telecom Design Control Document,” Revision A, July 18, 2005. JPL D-22724, Jet Propulsion Laboratory, California Institute of Technology, Pasadena, California.

[27]Lee, A., “Mars Reconnassance Orbiter Electra Baseband Processor Module (BPM) Modem Processor FPGA Specification”, May 4, 2006, Jet Propulsion Laboratory, California Institute of Technology, Pasadena, California, JPL D-26102 Rev. A

[28]Grigorian, E., Bruvold, K., Jedrey, T., and Lau, C., “BER Performance tests of MCAS Receiver”, Interoffice Memorandom Electra-02-012 (internal report), Jet Propulsion Laboratory, Pasadena, California, April 15, 2002.

[29]Justin Bradfield, Adam Crifasi, Norman Adam, “Carrier Acquisition and Tracking for Europa Relay Communications,” IEEE Aerospace Conference 2018, March 2018, Big Sky, Montana.

[30]Stephens, S. A., and Thomas, J. B., "Controlled-root formulation for digital phase-locked loops," *IEEE Transactions on Aerospace and Electronic Systems*, vol. 31, no. 1, pp. 78-95, Jan. 1995. doi: 10.1109/7.366295